UDC 681.586.2
doi:10.31799/1684-8853-2022-4-20-28

Articles

Signal processing of capacitive force sensors installed in the foot of an anthropomorphic robot

K. D. Krestovnikov[a], *Junior Researcher, orcid.org/0000-0001-6303-0344*
A. A. Erashov[a], *Junior Researcher, orcid.org/0000-0001-8003-3643, erashov.a@iias.spb.su*
[a]*St. Petersburg Federal Research Center of the RAS, 39, 14th Line, 199178, Saint-Petersburg, Russian Federation*

Introduction: *The force-moment sensing of the functional surfaces in robots based on compact capacitive force sensors can significantly improve interaction with the environment and humans. Capacitive force sensors provide high measurement accuracy and speed, but the electromagnetic interference can affect significantly the signal. When processing signals the influence of external noise must be taken into account, which increases the computation time.* ***Purpose:*** *To apply the developed interface circuit for processing signals from capacitive primary force transducers in a real-world robot.* ***Results:*** *Experimental verification of the developed solutions implied simulation of a step of the pedipulator of an anthropomorphic robot with the calculation of the coordinates of the center of pressure exerted on the foot with the four installed capacitive sensors. Software filtering and measuring capabilities of the microcontroller made it possible to achieve a signal-to-noise ratio of approximately 62.24 dB, which allows a closed-loop control system to function correctly. The average time for calculating the coordinates of the center of pressure on the foot with software filtering of the signal on the on-board computer of the robot was from 3.1 to 6.1 ms and meets the requirements for the sensory system of a walking robot.* ***Practical relevance:*** *The interface circuit allows to scale the number of connected primary force transducers, while software processing allows to normalize transducer signals by applying the calculated correction factors. Proposed solutions can be used in different robotic systems for real-time force measurement.*

Keywords *— force sensors, capacitive sensors, humanoid robots, robotic sensing system, digital signal processing*

For citation: Krestovnikov K. D., Erashov A. A. Signal processing of capacitive force sensors installed in the foot of an anthropomorphic robot. *Informatsionno-upravliaiushchie sistemy* [Information and Control Systems], 2022, no. 4, pp. 20–28. doi:10.31799/1684-8853-2022-4-20-28

Introduction

The implementation of sensor systems of force-moment sensing into robotic systems makes it possible to improve their interaction with the environment and humans, which is currently an urgent scientific task. Anthropomorphic robots are one of the rapidly developing areas in robotics that require force-moment sensing. Implementation of gait and balance are actual basic tasks of anthropomorphic robotics. Stable gait of walking robots with constantly maintained balance on uneven surfaces requires information about the position of the zero moment point (ZMP) [1], as well as information about the distribution of pressure over the supporting surface of the robot foot. The robot's control system receives this information from the sensor system, which consists of sensors, interface circuits and computing devices. The quality of maintaining the balance and gait of the robot depends on the accuracy and processing speed of the sensor system. Its performance largely depends on the used communication interfaces, computing devices and software. The accuracy of the received data is influenced by the parameters of sensitivity, static and cyclic drift of the sensors, and the quality of the interface circuit.

Force-torque sensors for controlling the gait of robots can be placed in the intermediate joints of the robot foot [2, 3], as well as on the surface of the foot, which is in direct contact with the supporting surface [4, 5].

The first method of installing sensors is used in [2], where six-axis force sensors were used to control the gait of the anthropomorphic robot. For high-level operations on board the robot, an on-board computer is used. The functions of the lower-level control systems are performed by Infineon C167-CS microcontrollers. Controllers and on-board computer communicate via CAN bus. A similar method of installing force sensors was used in the feet of the anthropomorphic robot BHR-2 [3]. To process signals from the pedipulator sensors, a signal processor (DSP) is used, one of the ADC inputs of which receives a signal from a force sensor. CAN bus is used for communication between control devices. In further developments [6], the same method of installing force-torque sensors in the feet of the BHR-5 robot was chosen. Similar to the BHR-2 robot, the interface circuit of the sensor is installed in each foot of the pedipulators. RS422 is selected as the communication inter-face between the measuring circuit and the sensors, the PCI interface is used to exchange data with a PC running RTLinux. As the authors note, the modules of the developed system communicate in real time with a period of 2 ms.

In the pedipulators of the anthropomorphic LOLA robot, a cruciform six-axis force-torque sensor is installed between the foot and ankle [7]. Each beam of the cross contains one strain gauge

sensor. The lower-level controllers are responsible for data processing. They are represented by signal processors that transmit the processed data to the upper-level controller under the control of the QNX system. The controllers exchange data via a communication system Sercos-III based on Ethernet.

In the ankle joints of the pedipulators of robots KHR-2 [8] and KHR-3 [9] force-torque sensors are used to determine ZMP while the anthropomorphic robot is walking. The frequency of sending data from the sensors is 10 ms, the control cycle of the servo drives is 1 ms. An on-board computer running Windows XP with RTX (Real Time eXtension) generates control signals with a period of 10 ms.

The second method of placing the sensors is structurally simpler, since it does not require the installation of an intermediate link in the pedipulator and makes it possible to determine the distribution of contact forces along the foot of the robot. For walking robot sensing [4], the resistors located at the corners of the foot of a rectangular shape are used. The resistance of these sensors changes depending on the magnitude of the applied external force. On the foot of each pedipulator there are 4 such sensors, the signals of which are read by the ADC of the ATMEGA 128 microcontroller. The controller also calculates the ZMP of the foot, after which it transmits the data to the remote computer using the RS-485 interface. To filter the signals from the sensors, a third-order Chebyshev low-pass filter is used. Similarly, force sensors installed in the feet of the robot are used in [5, 10]. The signals from the sensors are converted using an ADC with a 10 ms sampling time. Measurements are performed in real time on a PC running the RTLinux operating system. As a force sensor for determining ZMP in [11] a piezoresistive strain gauge is used. As in the works mentioned above, the four sensors are installed on each foot of the robot at its corners.

To calculate the ZMP, a combination of several methods of measuring the forces applied to the robot pedipulator is possible. Thus in [12], the authors combine sensors installed on the surface of the foot and in the ankle of the robot. As well, in [13], the authors propose a combination of fluid pressure sensors in the drives and force sensors installed at the corners of the robot's foot.

In contrast to the works discussed above, the matrix sensor [14] covers the entire foot surface of the H7 anthropomorphic robot pedipulators. The signal from the matrix sensor is measured with a period of 1 ms; an operational amplifier with an ADC is used as an interface circuit. The digitized data is transferred via the USB interface to a PC running RTLinux. A matrix of tensoresistive sensors with a dimension of 8×10 cells, covering the entire surface of the foot, is also used in [15].

Based on the analysis performed, as well as the data presented in the works [16–18], the time for obtaining data from the sensors and calculating the center of applied pressure area to the foot should be in the range of up to 10 ms for the robot's control system to respond sufficiently and to create a stable gait.

Installing force sensors directly on the foot surface, which contacts with the ground makes it possible to obtain information about the distribution of forces within the support area of the robot's feet and information about the properties of the supporting surface. Such primary force transducers are thin, so they do not affect robot's gait. This solution is easily scalable and can be effectively used in walking robots of medium and small size. The analysis of solutions described above showed that most of them are based on tensoresistive sensors with a film structure. The disadvantages of film strain gauges are high static and cyclic drift and a relatively short service life. In [19], we proposed a structure of sensor based on the capacitive principle, which do not have such disadvantages. In this work, we continue our research towards the use of capacitive force sensors in the foot of the anthropomorphic robot, with a focus on processing sensor signals. This work offers a comprehensive assessment of the practical application of the proposed sensors of our own design as part of the robotic system. The advantage of our work is that we do not consider individual tests of sensors with potential application in robotics, but test them on a real robot and process data from them for further use by the control system.

Circuit solutions of the sensors

In [19], we described in detail the structure of a capacitive primary transducer of pressure force and proposed some design ratios and an interface circuit for converting a signal into a dependence of voltage on the applied pressure force. The next stage of research was the development of a matrix of pressure force sensors based on the proposed sensor structure. The application of the interface scheme proposed in [19] for the matrix required a separate adjustment of each cell, which requires a significant amount of time. In [20], we proposed an interface circuit based on an operational amplifier, which requires tuning one matrix cell, and for the rest, the same component ratings are used. The disadvantage of the interface scheme described in [20] was that after adjusting the sensor the output signal from the interface circuit could change in a small range. This feature does not allow using the entire range of ADC values of the microcontroller, which negatively affects the accuracy of force measurement. In order to use the full range of ADC values, we have added

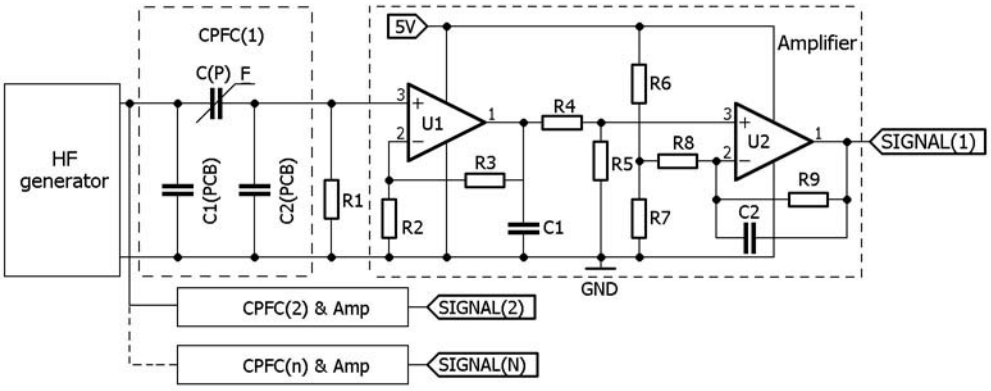

■ ***Fig. 1.*** Interface circuit of capacitive force sensors

a differential amplifier to our circuit design. A new schematic diagram for converting a capacitive primary force converter (CPFC) signal into a voltage is shown in Fig. 1.

The principle of operation of the CPFC is based on a change in the distance between the electrodes of the cell, which changes in direct proportion to the applied force. When an external force is applied to the CPFC, its capacitance changes and, accordingly, the reactance changes as well. Since $C(P)$ and R_1 form a divider, changes in reactance $C(P)$ change the voltage applied to the noninverting input of the op-amp. A noninverting amplifier is built on U_1. Its gain is determined by the ratio of R_3 and R_2. The output signal from U_1 smoothed by C_1 is fed to the input of a differential amplifier built on U_2. The divider R_6R_7 forms the dead zone U_2, thereby excluding the DC component from the output signal of the sensor, which corresponds to the level of the output voltage from U_1 in the absence of an external force applied to the CPFC. Also, with the help of R_6R_7, it is possible to form a sensor dead zone at the beginning of the force measurement range. The amplification factor of the signal difference U_2 is determined based on the equation

$$k = R_5 / R_4, \quad (1)$$

where $R_5 = R_9$ and $R_4 = R_8$.

By changing the gain U_2, it is possible to increase the sensor's sensitivity relative to the value obtained after adjusting the gain U_1 and selecting R_1. The process of setting up the interface circuit without a differential amplifier and the calculated ratios are presented in detail in [20].

During experiments, four identical sensors were installed on the foot of the anthropomorphic robot. A significant interference in their output signals occurred, induced by servo drives and other robot electronics. To filter this noise, a capacitor C_2 was added to the feedback U_2, so the operational amplifier began to perform the function of a low-pass

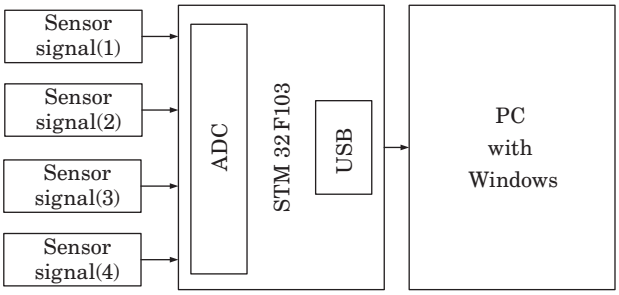

■ ***Fig. 2.*** Block diagram of the connection of force sensors in the foot of the anthropomorphic robot

filter with a cutoff frequency of 15 Hz. The filter cutoff frequency was selected based on our experiments on gait simulation and the capabilities of the robot's mechanical subsystem. For robots in which the force applied to the foot can change at a frequency of more than 15 times per second, a higher cutoff frequency should be selected. The block diagram of connecting sensors to the robot's computing system is shown in Fig. 2.

The signals from the sensors are read out by means of a 12-bit microcontroller ADC, and then the received data is sent via the USB interface to the on-board computer of the robot for further processing.

Software processing of the sensors signals

Experiments with the developed sensor matrix of a similar design described in [20] showed that the levels of the output signals of the cells of the sensor matrix differ from each other. This feature is mainly associated with the imperfect manufacturing of the sensor itself. The deformable spacer may differ in thickness over the area of the matrix, which leads to differences in the capacities of the cells. The situation is similar with individual sensors installed in the foot of the robot. For correct subsequent calcu-

lations, normalization of sensors signals on primary signal processing level is required. The introduction of normalizing coefficients allows obtaining identical data from each of the sensors. We propose to use the following approach for this.

Sensors may differ from each other in sensitivity and in the initial level of the output signal. In the general case, the sensor output signal can be described by an equation of the straight form $y = kx + \Delta$. Thus, in order to bring the signals from each of the sensors to the same level, it is necessary to derive two correction factors k and Δ. To calculate Δ it is necessary to calculate the average level for the output signals E_{av}:

$$E_{av} = \sum_{i=1}^{n} E_i / n, \quad (2)$$

where n is the number of force sensor cells; E_i is the level of the output signal from each sensor in absence of external load.

Next, the correction value Δ_i is calculated for the output signal of each cell of the matrix:

$$\Delta_i = E_{av} - E_i. \quad (3)$$

Then, with a fixed equal force applied to all sensors, the proportional factor k_i is calculated for each sensor:

$$k_i = \frac{E_{av\_new} + \Delta_i}{E_{if}}, \quad (4)$$

where E_{av_new} is determined by (2) the average value of the output signal from the sensors at a fixed applied force and E_{if} is the output from the sensor cell when an external force is applied to it.

The normalized value of the signal from each sensor is determined by the following expression:

$$E_{i\_new} = k_i E_i + \Delta_i. \quad (5)$$

The introduction of these correction factors improves quality of the high-level software signal processing for the developed sensors.

To calculate the coordinates of the center of pressure (CoP) on the foot, one can use the following equations derived in [21]:

$$X_c = \frac{\sum_{i=1}^{N} X_i F_i}{\sum_{i=1}^{N} F_i}, \quad (6)$$

where X_i is the abscissa of the point of application of force to each support of the foot; F_i is the force applied to each support of the foot, and N it is the number of points to which the force is applied;

$$Y_c = \frac{\sum_{i=1}^{N} Y_i F_i}{\sum_{i=1}^{N} F_i}, \quad (7)$$

where Y_i is the ordinate of the point where the force is applied to each support of the foot. The proposed equations (6), (7) make it possible to calculate CoP for any number of sensors installed in arbitrary places on the robot's foot.

In accordance with the approach described above, the normalizing coefficients are calibrated according to equations (2)–(4), which are then stored in the memory of the on-board computer of the anthropomorphic robot. After that, it is possible to further receive data on the force from the microcontroller, normalize signals from each sensor according to equation (5) and process the obtained values. The result of applying the proposed approach is the coordinates of the center point of the applied pressure for each foot of the robot.

Experiments and results

The proposed solutions were implemented on one pedipulator of a small-sized anthropomorphic robot with a total mass about 7 kg [22, 23]. The appearance of the prototype's foots are shown in Fig. 3.

The robot's foot has four reference points at each of which a sensor is installed, forming a trapezoid. Like a human foot, the forefoot of the robot can bend up to 39.5° and it is wider than the heel. Fig. 4 shows the appearance of the assembled printed circuit board, which implements the new interface circuit proposed in this work and two CPFC. These boards are installed on the toe and heel of the pedipulator foot.

Software for processing data from foot sensors and visualization CoP were developed. Fig. 5 shows frames from the video [24], which demonstrates the movement of the pedipulator's foot from the state of full support on the surface to the state of support on the toe, as a result of which CoP also moves. In Fig. 5, CoP is shown with a red dot. Video [25] also demonstrates the CoP displacement to one of the four foot supports when force is applied to each sensor cell separately.

In the experiments, the median filter was used due to its computational simplicity and speed of operation [26], as well as the measurement capabilities of the ADC of the STM32F103C8T6 microcontroller.

The data for evaluating the noise were obtained as a result of measuring the signals from the sensors in the absence of external force and servo drives in the pedip-

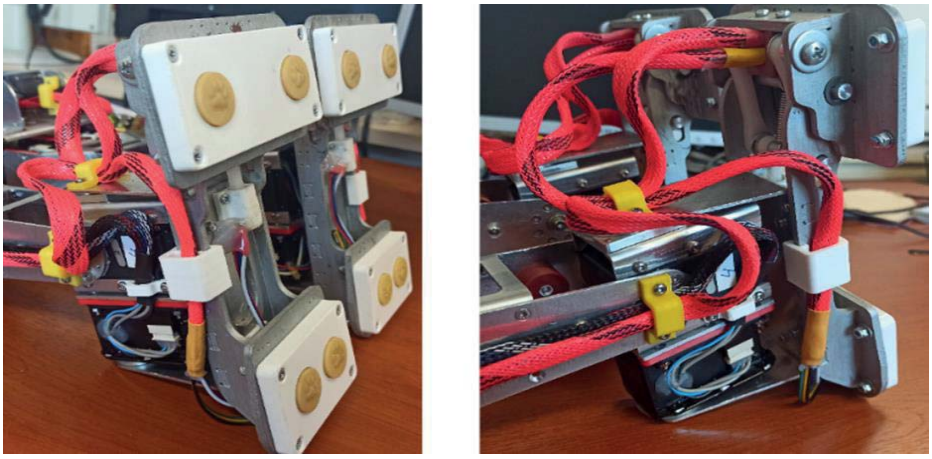

■ ***Fig. 3.*** The feet of the anthropomorphic robot

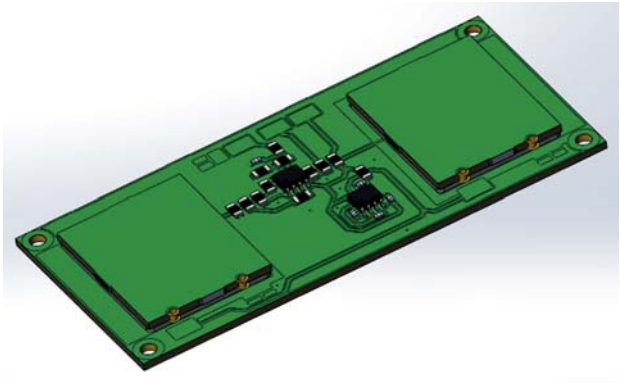

■ ***Fig. 4.*** Sensors used in the foot of the anthropomorphic robot

ulator operating in mode of holding the moment. Three options for processing signals from sensors were considered: *case A* is measurements with a combination of increased ADC sampling time and median filter, *case B* is the measurements with increased sampling time (ADC parameter cycles is 7.5), *case C* is the measurements without filtering (cycles is 1.5). After the experiments, more than 100,000 values were obtained for each sensor in the foot. For each case under consideration, the standard deviations (STD) and average (AVG) values in the ADC values were calculated (Table).

It follows from Table that the filtering allows to reduce the level of noise in the output signals from the sensors. The use of a median filter with an increased sampling time of the ADC made it possible to reduce the noise level by an average of ≈ 5.33 times, while the maximum difference in the signals from the sensors was ≈ 33 %, and for the case without filtration ≈ 53 %.

The following series of experiments were carried out to evaluate the cumulative performance of the interface circuit computing system and the CPFC. For robotic control systems, an important parameter affecting the quality of work is time of receiving and processing data from the sensor system. The parameter of the total time for receiving and processing data is made up of the following time intervals:

$$t_s = t_{reaction} + t_M + t_{transfer} + t_{processing}, \qquad (8)$$

where $t_{reaction}$ is the sensor response time and delay time from the operational amplifier; t_M is the cycle time of the microcontroller; $t_{transfer}$ is the time of data transfer over the communication interface, and $t_{processing}$ is time of data processing: normalization and calculation of the coordinates of the center of pressure.

Simulation of 10 steps of the pedipulator was performed with the force of foot pressure on the surface of 35 N. The process of simulation a step is shown in Fig. 6 [27].

In these experiments the total run time of each cycle of the microcontroller was measured using the built-in Data Watchpoint and Trace unit (DWT). The average cycle time of the microcontroller was t_M = 0.105 ms. It is worth noting that increasing the ADC sampling time does not significantly affect the overall cycle time of the microcontroller. According to the formula given in the documentation [28], measurement time increases from ≈ 1.167 μs to ≈ 1.429 μs, with cycles equal 1.5 and 7.5 respectively.

Time of data transfer from the microcontroller $t_{transfer}$ was obtained by measuring the time for performing the request-response operation on the on-board computer. The on-board computer sends a request to the microcontroller to receive a message with data on the force applied to each sensor. After receiving a response, the on-board computer records the time. Thus, $t_{transfer}$ is assumed to be equal to half of the time required for the request-response operation, and ranges approximately from 2 to 5 ms. Experiments with determining the point of the center of pressure of the foot showed that the use

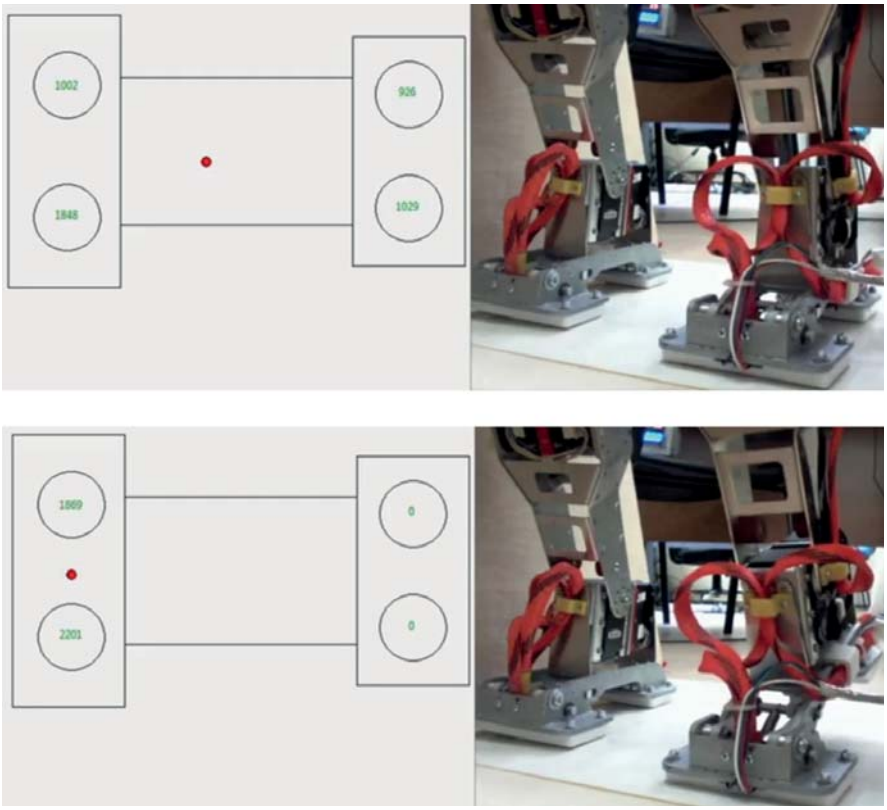

■ ***Fig. 5.*** Visualization of CoP at the different foot positions

■ Deviations of the sensor signals and the signal to noise ratio

Parameter	Case	Sensor 1	Sensor 2	Sensor 3	Sensor 4	AVG
STD (ADC values)	A	2	2	3	2	2.25
	B	6	11	8	8	8.25
	C	11	19	9	9	12
Signal to noise ratio, dB	A	63.74	63.48	59.09	62.66	62.24
	B	57.41	48.49	52.21	53.43	52.89
	C	47.46	42.79	49.37	49.20	47.21

of the median filter had little effect on the signal processing time on the on-board computer. Using Python software, average time $t_{processing}$ for each case was ≈ 1 ms. Average time of calculating the coordinates of the center of pressure point t_s (8), considering the fact that the response time of each sensor is much less than the time of measurement by the microcontroller, as well as data transfer to the on-board computer and their processing, corresponds to the range from 3.1 to 6.1 ms. According to the results of the above analysis, the value of the CoP calculation time interval obtained using the sensors we proposed meets the requirements for the sensor system for the implementation of stable gait algorithms for anthropomorphic robots. The calculated values of the points of the center of pressure in the process of simulating the step of the pedipulator for different cases of signal filtering are shown in Fig. 7. The points are shown as deviations from the geometric center of the foot.

To determine the real CoP, 4 special platforms with tensoresistive sensors were installed in the experimental stand, on which the pedipulator stepped in the process of simulating a step (see Fig. 6). The measured forces in accordance with (6) and (7) were used to calculate the actual CoP value and are depicted by the symbol "×" in Fig. 7. As can be seen from the graph, the using of the median filter and the increased sampling time of the ADC allowed us to obtain CoP values closer to real ones. In this case,

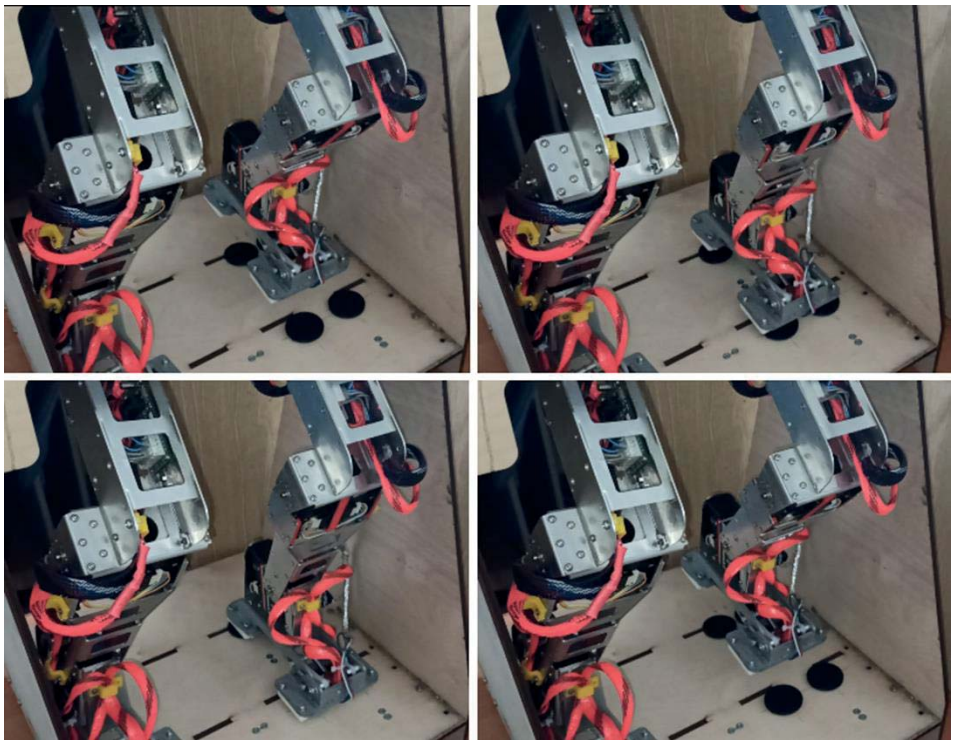

■ ***Fig. 6.*** The one step of the pedipulator

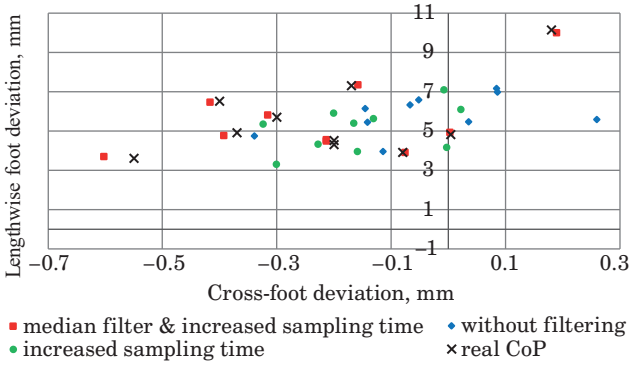

■ ***Fig. 7.*** Average values of the center of pressure on the robot foot at 10 steps

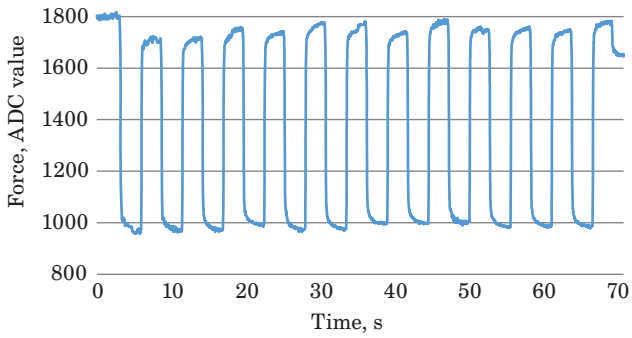

■ ***Fig. 8.*** The change in force from one of the sensors when using a median filter and an increased ADC sampling time

on average, a deviation of ≈ 0.016 mm was obtained for the coordinates along the X-axis and 0.086 mm for the coordinates along the Y-axis.

The largest deviation between the points of the center of the applied pressure to the foot corresponds to ≈ 6.3 mm along the Y-axis, while the deviation was ≈ 4.5 % of the foot length. The scatter of points is affected by the inaccuracy of the positioning of the links and their non-rigidity, as well as backlash in the joints, which is confirmed by the graph of the simulation of steps in Fig. 8.

The graph in Fig. 8 corresponds to the signal from one of the sensors on the toe of the foot after using the median filter and the increased sampling time of the ADC. It can be seen, that the force applied to the sensor during the simulation of step was uneven, which confirms the above assumptions.

Conclusions

The paper presents the implementation of self-developed capacitive force sensors into the feet of a small-sized anthropomorphic robot. The offered force sensors are installed on the surface of the foot and allow calculating the center of applied pressure to the foot. The received data from the sensors can be used to calculate the ZMP [29]. An approach for primary

software signal processing has been developed, which allows reducing the difference in the characteristics of the sensors, occurring due to imperfections of CPFC manufacturing. The presented interface circuit with a differential amplifier allows one to use the entire ADC range and to increase the CPFC sensitivity.

During the experiments, the noise characteristics of the sensory system of the foot were considered when implementing various methods of filtering signals. The increase of sampling time of the ADC of the microcontroller in combination with the median filter allows obtaining an average signal-to-noise ratio of ≈ 62.24 dB without significant delays in signal processing.

The fundamental parameter for the correct operation of the system when the robot maintains balance or the implementation of a stable gait is the duration of the control cycle. This parameter is highly dependent on the speed of the sensor system. The average time for obtaining the coordinates of the center of pressure is in the range from 3.1 to 6.1 ms, which meets the requirements for cycle time of gait control systems for walking robots. The computation time can be reduced by using faster programming languages in the high-level part. In addition, real-time systems like QNX can achieve 2 ms USB transfer times without unpredictable delays.

The results obtained in the article show that the proposed solution can be applied in walking robots, including anthropomorphic ones for the implementation of stable gait algorithms. Besides the using of developed solutions can have significant influence on development of cyber-physical systems and collaborative robotics [30].

References

1. Kovalev A., Pavliuk N., Krestovnikov K., Saveliev A. Generation of walking patterns for biped robots based on dynamics of 3D linear inverted pendulum. *Intern. Conf. on Interactive Collaborative Robotics*, Aug. 2019, pp. 170–181. doi:10.1007/978-3-030-26118-4_17
2. Gienger M., Loffler K., Pfeiffer F. Towards the design of a biped jogging robot. *Proc. ICRA, IEEE Intern. Conf. on Robotics and Automation*, May 2001, vol. 4, pp. 4140–4145. doi:10.1109/ROBOT.2001.933265
3. Li J., Huang Q., Zhang W., Yu Z., Li K. Flexible foot design for a humanoid robot. *IEEE Intern. Conf. on Automation and Logistics*, 2008, pp. 1414–1419. doi:10.1109/ICAL.2008.4636375
4. Choi K. C., Lee H. J., Lee M. C. Fuzzy posture control for biped walking robot based on force sensor for ZMP. *SICE-ICASE Intern. Joint Conf.*, 2006, pp. 1185–1189. doi:10.1109/SICE.2006.315363
5. Erbatur K., Okazaki A., Obiya K., Takahashi T., Kawamura A. A study on the zero moment point measurement for biped walking robots. *IEEE 7th Intern. Workshop on Advanced Motion Control. Proc.*, July 2002, pp. 431–436. doi:10.1109/AMC.2002.1026959
6. Yu Z., Huang Q., Ma G., Chen X., Zhang W., Li J., Gao J. Design and development of the humanoid robot BHR-5. *Advances in Mechanical Engineering*, 2014, 6, p. 852937. https://doi.org/10.1155/2014/852937
7. Lohmeier S., Buschmann T., Ulbrich H. Humanoid robot LOLA. *IEEE Intern. Conf. on Robotics and Automation*, 2009, pp. 775–780. doi:10.1109/ROBOT.2009.5152578
8. Kim J. Y., Park I. W., Oh J. H. Experimental realization of dynamic walking of the biped humanoid robot KHR-2 using zero moment point feedback and inertial measurement. *Advanced Robotics*, 2006, vol. 20(6), pp. 707–736.
9. Park I. W., Kim J. Y., Oh J. H. Online walking pattern generation and its application to a biped humanoid robot – KHR-3 (HUBO). *Advanced Robotics*, 2008, vol. 22(2-3), pp. 159–190. doi:10.1163/156855308X292538
10. Prahlad V., Dip G., Meng-Hwee C. Disturbance rejection by online ZMP compensation. *Robotica*, 2008, vol. 26(1), p. 9. doi:10.1017/S0263574707003542
11. Yasin A., Xu Q., Chen B., Lu Q., Khan M. W. Design of a 23-DoF small humanoid robot with ZMP force sensors. *Intern. Conf. "Informatics in Control, Automation and Robotics"*, 2011, pp. 31–38. doi:10.1007/978-3-642-25899-2_5
12. Erbatur K., Seven U., Taskiran E., Koca O., Kiziltas G., Unel M., Onat A. SURALP-L-The leg module of a new humanoid robot platform. *Humanoids 2008 – 8th IEEE-RAS Intern. Conf. on Humanoid Robots*, pp. 168–173. doi:10.1109/ICHR.2008.4755963
13. Hyon S. H., Suewaka D., Torii Y., Oku N., Ishida H. Development of a fast torque-controlled hydraulic humanoid robot that can balance compliantly. *IEEE-RAS 15th Intern. Conf. on Humanoid Robots (Humanoids)*, 2015, pp. 576–581. doi:10.1109/HUMANOIDS.2015.7363420
14. Kagami S., Takahashi Y., Nishiwaki K., Mochimaru M., Mizoguchi H. High-speed matrix pressure sensor for humanoid robot by using thin force sensing resistance rubber sheet. *IEEE Sensors*, 2004, pp. 1534–1537. doi:10.1109/ICSENS.2004.1426481
15. Shimojo M., Araki T., Ming A., Ishikawa M. A ZMP sensor for a biped robot. *Proc. IEEE Intern. Conf. on Robotics and Automation*, 2006, pp. 1200–1205. doi:10.1109/ROBOT.2006.1641872
16. Yang U. J., Kim J. Y. Mechanical design of powered prosthetic leg and walking pattern generation based on motion capture data. *Advanced Robotics*, 2015, vol. 29(16), pp. 1061–1079. doi:10.1080/01691864.2015.1026939
17. Gorobtsov A. S., Andreev A. E., Markov A. E., Skorikov A. V., Tarasov P. S. Features of solving the inverse

dynamic method equations for the synthesis of stable walking robots controlled motion. *SPIIRAS Proc.*, 2019, vol. 18(1), pp. 85–122 (In Russian). doi:10.15622/sp.18.1.85-122

18. Kim I. S., Han Y. J., Hong Y. D. Stability control for dynamic walking of bipedal robot with real-time capture point trajectory optimization. *Journal of Intelligent & Robotic Systems*, 2019, vol. 96(3), pp. 345–361. doi:10.1007/s10846-018-0965-7

19. Krestovnikov K., Saveliev A., Cherskikh E. Development of a circuit design for a capacitive pressure sensor, applied in walking robot foot. *IEEE 20th Mediterranean Electrotechnical Conf. (MELECON)*, 2020, pp. 243–247. doi:10.1109/MELECON48756.2020.9140509

20. Krestovnikov K., Erashov A., Bykov A. Development of circuit solution and design of capacitive pressure sensor array for applied robotics. *Robotics and Technical Cybernetics*, 2020, vol. 8(4), pp. 296–307 (In Russian). doi:10.31776/RTCJ.8406

21. Kajita S., Hirukawa H., Harada K., Yokoi K. *Introduction to humanoid robotics*. Ser. Springer Tracts in Advanced Robotics, vol. 101. Springer, Berlin, Heidelberg, 2014. 222 p. doi:10.1007/978-3-642-54536-8

22. Pavluk N., Ivin A., Budkov V., Kodyakov A., Ronzhin A. Mechanical leg design of the anthropomorphic robot Antares. *Intern. Conf. on Interactive Collaborative Robotics*, 2016, pp. 113–123. doi:10.1007/978-3-319-43955-6_15

23. Pavluk N., Denisov A., Kodyakov A., Ronzhin A. Mechanical engineering of leg joints of anthropomorphic robot. *MATEC Web of Conf.*, vol. 77, p. 04006, EDP Sciences, 2016. doi:10.1051/matecconf/20167704006

24. *Determination of the center of pressure of Antares' foot during stride*. Available at: https://www.youtube.com/watch?v=NoYQ1oqr84M (accessed 30 May 2022).

25. *Center of pressure of Antares foot at pressure on each sensor cell*. Available at: https://www.youtube.com/watch?v=zRU3VnGsblk (accessed 30 May 2022).

26. Pitas I., Venetsanopoulos A. N. Nonlinear digital filters: Principles and applications. Ser. The Springer International Series in Engineering and Computer Science, vol. 84. Springer Science & Business Media, 2013. 392 p. doi:10.1007/978-1-4757-6017-0

27. *Simulation of the step of the ANTARES pedipulator*. Available at: https://www.youtube.com/watch?v=qlh-5NHOwMK0 (accessed 30 May 2022).

28. *Medium-density performance line ARM®-based 32-bit MCU*. Available at: https://www.st.com/resource/en/datasheet/stm32f103c8.pdf (accessed 30 May 2022).

29. Sardain P., Bessonnet G. Forces acting on a biped robot. Center of pressure — zero moment point. *IEEE Transactions on Systems, Man, and Cybernetics — Part A: Systems and Humans*, 2004, vol. 34, no. 5, pp. 630–637.

30. Galin R., Shiroky A., Magid E., Meshcheryakov R., Mamchenko M. Effective functioning of a mixed heterogeneous team in a collaborative robotic system. *Informatics and Automation*, 2021, vol. 20, no. 6, pp. 1224–1253 (In Russian). doi:10.15622/ia.20.6.2

УДК 681.586.2
doi:10.31799/1684-8853-2022-4-20-28

Обработка сигналов емкостных датчиков силы, установленных в стопу антропоморфного робота

К. Д. Крестовников[a], младший научный сотрудник, orcid.org/0000-0001-6303-0344
А. А. Ерашов[a], младший научный сотрудник, orcid.org/0000-0001-8003-3643, erashov.a@iias.spb.su
[a]Санкт-Петербургский Федеральный исследовательский центр РАН, 14-я линия В. О., 39, Санкт-Петербург, 199178, РФ

Введение: основанное на компактных емкостных датчиках силы силомоментное очувствление функциональных поверхностей роботов позволяет существенно улучшить их взаимодействие с окружающей средой и людьми. Емкостные датчики силы обеспечивают высокую точность и скорость измерений, но электромагнитные помехи могут оказывать существенное влияние на их выходной сигнал. При последующей обработке сигналов должно учитываться влияние внешних помех, что увеличивает время вычислений. **Цель:** применить разработанную интерфейсную схему для обработки сигналов от емкостных первичных преобразователей силы в реальном роботе. **Результаты:** экспериментальная проверка разработанных решений заключалась в моделировании шага педипулятора антропоморфного робота с расчетом координат центральной точки давления на стопу с установленными четырьмя емкостными датчиками. Программная фильтрация и измерительные возможности микроконтроллера позволили добиться отношения сигнал/шум примерно 62,24 дБ, что дает возможность замкнутой системе автоматического регулирования корректно функционировать. Среднее время расчета координат центра давления на стопу при программной фильтрации сигнала на бортовом компьютере робота составило от 3,1 до 6,1 мс, что соответствует требованиям к сенсорной системе шагающего робота. **Практическая значимость:** интерфейсная схема имеет возможность масштабировать количество подключаемых первичных преобразователей силы, а программная обработка позволяет нормировать сигналы преобразователей путем применения рассчитанных поправочных коэффициентов. Предлагаемые решения могут быть использованы в различных робототехнических системах для измерения силы в режиме реального времени.

Ключевые слова — датчики силы, емкостные датчики, гуманоидные роботы, сенсорная система робота, цифровая обработка сигналов.

Для цитирования: Krestovnikov K. D., Erashov A. A. Signal processing of capacitive force sensors installed in the foot of an anthropomorphic robot. *Информационно-управляющие системы*, 2022, № 4, с. 20–28. doi:10.31799/1684-8853-2022-4-20-28
For citation: Krestovnikov K. D., Erashov A. A. Signal processing of capacitive force sensors installed in the foot of an anthropomorphic robot. *Informatsionno-upravliaiushchie sistemy* [Information and Control Systems], 2022, no. 4, pp. 20–28. doi:10.31799/1684-8853-2022-4-20-28